Title

Endovascular MR-guided Renal Embolization by Using a Magnetically Assisted Remote-controlled Catheter System.

Permalink

https://escholarship.org/uc/item/12s3c805

Journal

Radiology, 281(1)

ISSN

0033-8419

Authors

Lillaney, Prasheel V
Yang, Jeffrey K
Losey, Aaron D
et al.

Publication Date

2016-10-01

DOI

10.1148/radiol.2016152036

Peer reviewed

Radiology

Endovascular MR-guided Renal Embolization by Using a Magnetically Assisted Remote-controlled Catheter System[1]

Prasheel V. Lillaney, PhD
Jeffrey K. Yang, BS
Aaron D. Losey, MD
Alastair J. Martin, PhD
Daniel L. Cooke, MD
Bradford R. H. Thorne
David C. Barry, BS
Andrew Chu, BA
Carol Stillson, DVM
Loi Do, MS
Ronald L. Arenson, MD
Maythem Saeed, DVM, PhD
Mark W. Wilson, MD
Steven W. Hetts, MD

Purpose: To assess the feasibility of a magnetically assisted remote-controlled (MARC) catheter system under magnetic resonance (MR) imaging guidance for performing a simple endovascular procedure (ie, renal artery embolization) in vivo and to compare with x-ray guidance to determine the value of MR imaging guidance and the specific areas where the MARC system can be improved.

Materials and Methods: In concordance with the Institutional Animal Care and Use Committee protocol, in vivo renal artery navigation and embolization were tested in three farm pigs (mean weight 43 kg ± 2 [standard deviation]) under real-time MR imaging at 1.5 T. The MARC catheter device was constructed by using an intramural copper-braided catheter connected to a laser-lithographed saddle coil at the distal tip. Interventionalists controlled an in-room cart that delivered electrical current to deflect the catheter in the MR imager. Contralateral kidneys were similarly embolized under x-ray guidance by using standard clinical catheters and guidewires. Changes in renal artery flow and perfusion were measured before and after embolization by using velocity-encoded and perfusion MR imaging. Catheter navigation times, renal parenchymal perfusion, and renal artery flow rates were measured for MR-guided and x-ray–guided embolization procedures and are presented as means ± standard deviation in this pilot study.

Results: Embolization was successful in all six kidneys under both x-ray and MR imaging guidance. Mean catheterization time with MR guidance was 93 seconds ± 56, compared with 60 seconds ± 22 for x-ray guidance. Mean changes in perfusion rates were 4.9 au/sec ± 0.8 versus 4.6 au/sec ± 0.6, and mean changes in renal flow rate were 2.1 mL/min/g ± 0.2 versus 1.9 mL/min/g ± 0.2 with MR imaging and x-ray guidance, respectively.

Conclusion: The MARC catheter system is feasible for renal artery catheterization and embolization under real-time MR imaging in vivo, and quantitative physiologic measures under MR imaging guidance were similar to those measured under x-ray guidance, suggesting that the MARC catheter system could be used for endovascular procedures with interventional MR imaging.

© RSNA, 2016

Radiology

Minimally invasive, image-guided interventions are most often performed with x-ray fluoroscopy, especially in endovascular interventions wherein high spatial and temporal resolution is necessary. Magnetic resonance (MR) imaging has emerged as a complementary imaging modality to x-ray and becomes an attractive alternative to x-ray when soft-tissue characteristics or other physiologic information (eg, tissue perfusion) is required to successfully complete the intervention (1–4). Several research groups have engineered methods to perform interventions solely with MR imaging (5–14). However, endovascular interventions in these studies involve navigating the cardiac chambers or relatively large abdominal aortic vessels due to the lack of commercially available MR-compatible guidewires analogous to the metallic guidewires used in x-ray–guided endovascular navigation. The absence of MR-compatible guidewires generally prevents safe access to smaller and more tortuous vessels.

Two broad approaches are being developed to improve catheter navigation capabilities by using MR guidance: those that enhance visualization and ability to track the interventional device (15–19) and those that enhance the steerability of the interventional device through mechanical (20), hydraulic

(21), shape memory polymer (22), or magnetic means. The magnetic approach leverages an interaction with the main magnetic field (B_0) or gradient fields (G) and can use rare earth permanent magnet beads (23,24) or a microcoil (25). The magnetically assisted remote-controlled (MARC) catheter, developed by our group, interacts with B_0 and uses microcoils. By running a current through the microcoil, a magnetic moment is created that will prefer to align with the direction of B_0 causing the catheter tip to deflect. The MARC system has several advantages: the microcoil can be switched off when desired, the current to the microcoil can be finely tuned, the microcoils can be miniaturized thus minimizing the diameter of the catheter tip, and costs for mass production of the microcoils are likely to be low.

Previous studies with the MARC catheter system have focused on in vitro navigation in one or two planes and evaluation of in vivo safety with regard to tissue damage from resistive or radiofrequency heating (26–28). The aims of our preclinical study are twofold, while advancing toward the goal of translating the MARC catheter system for clinical use: to assess the feasibility of the MARC catheter system under MR imaging guidance for performing a simple endovascular procedure (ie, renal artery embolization) in vivo and to compare with x-ray guidance

to determine the value of MR imaging guidance and the specific areas where the MARC system can be improved.

Materials and Methods

MARC Catheter System Design

An in-kind donation of raw materials and expertise in manufacturing the custom catheter body was provided by Penumbra (Alameda, Calif). The novel MARC catheter tip was built in-house at the University of California, San Francisco. Authors who are not employees of Penumbra were in total control of the analysis and inclusion of the data. R.L.A. is one of the inventors of the MARC catheter system (U.S. Patent 6304769). The MARC catheter prototype used in our study had a saddle-shaped microcoil embedded on a 1.2-mm–diameter hollow alumina tip (Fig 1a, 1b). The saddle design was composed of two virtually identical coil patterns, with one pattern on each side of the cylindrical tip fabricated by laser lithography (P.V.L.L), as previously described (29,30). Electrical connections to the microcoil were made by using a pair of 0.125-mm–diameter copper wires embedded in the catheter wall (P.V.L.). The pair of copper wires was connected to 500 × 500-μm copper pads at the center of the coil pattern

Advances in Knowledge

- Use of the magnetically assisted remote-controlled (MARC) catheter system for swine renal artery catheterization and embolization under real-time MR guidance is feasible and comparable to standard x-ray guided intervention.

- MR guidance allowed timely intraprocedural quantitative assessment of renal perfusion and blood flow both before and after embolization.

- Due to current-dependent magnetic field distortion, the MARC catheter tip position is easily visible under MR imaging guidance in vivo.

Implications for Patient Care

- MR-guided interventions provide intraprocedural soft-tissue and physiologic information not available with x-ray guidance alone; these data can provide quantitative measures of success or complications.

- Although multimodality x-ray and MR imaging combination interventional suites are rare, evaluation of techniques in these suites will determine which procedures can benefit from unimodal (x-ray or MR imaging) or multimodal (combined x-ray and MR imaging) guidance.

Radiology

Figure 1: MARC catheter coil design. Each coil pattern consists of 13 turns of copper separated by a 50-μm pitch distance, a 500 × 5000-μm copper pad to attach interconnects, and a copper trace connecting the two coils to each other.

by using conventional microsoldering. These custom catheters (1.2-mm distal outer diameter) were prototypes provided as an in-kind donation by Penumbra. The prototypes were similar to commercially available PX Slim (Penumbra) neurovascular microcatheters except the standard metallic braiding was replaced with current-carrying copper wires. The completed microcoil tip was attached (P.V.L.) to the custom catheter shafts by using medical-grade polyester heat shrink tubing (Advanced Polymers, Salem, NH) as shown in Figure 1c.

To perform a procedure effectively inside the MR suite, a control system consisting of an MR imaging–safe cart and computer running a custom (LabVIEW; National Instruments, Austin, Tex) interface was developed (P.V.L.,

A.D.L., B.R.H.T.) to allow the interventionalist control, via foot pedals, value, and polarity of the current delivered to the microcoil tip (30,31). Additionally, the interventionalist was able to turn the current on and off with the foot pedal actuator. The control system cart was positioned in the MR imaging suite between the 5-gauss and 30-gauss lines. No discernible force was detected on the cart at this distance.

Animal Preparation Protocol

The study (Animal Care and Use Committee protocol AN103047–02A) was performed in concordance with the *Guide for the Care and Use of Laboratory Animals* (32), and approval was obtained from the institutional committee on animal research. Three swine

(mean weight, 43 kg ± 2) were obtained (Pork Power Farms, Turlock, Calif) and acclimatized locally for 48 hours prior to experiments. Animals were placed under general anesthesia (M.S., C.S.). Oxygen saturation levels of the animals were continuously monitored during the procedure, and cardiac monitoring was performed during MR pulse sequences that required cardiac gating. Prior to percutaneous femoral access, the animals received 0.2 mL per kilogram of body weight of heparin (Heparin Sodium Injection; Fesenius Kabi, Lake Zurich, Ill).

Imaging and Catheterization Protocol

All experiments were performed in a clinical hybrid interventional x-ray and MR imaging facility that includes both

Radiology
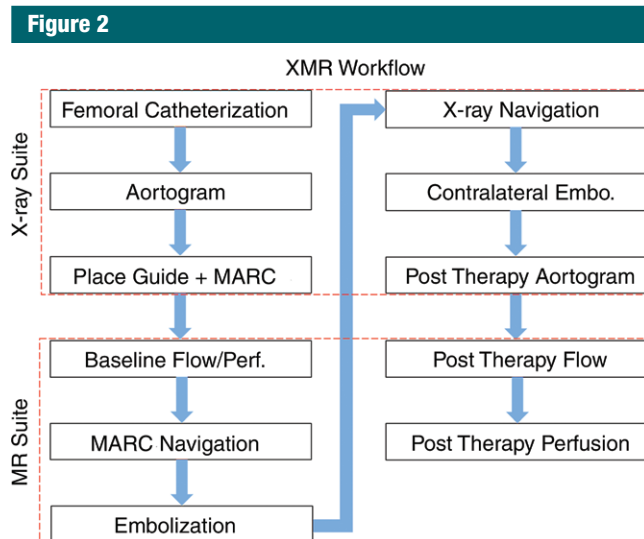
Figure 2: Imaging and intervention workflow in the x-ray and MR suite.

an Achieva 1.5-T MR imager (Philips Healthcare, Best, the Netherlands) and an Integris V5000 C-arm digital subtraction angiography (DSA) system (Philips Healthcare) positioned in-line in an adjoining dual-suite configuration. The two imaging modalities are connected by using a floating patient table that enables transferring the imaging subject between the modalities in a few minutes. The imaging workflow for the entire intervention is shown in Figure 2.

For each animal, catheterization was initially performed by three interventionalists (S.W.H. with 13 years, D.L.C. with 9 years, and M.W.W. with 20 years of experience with conventional endovascular procedures) in the C-arm suite. A 3.67-mm arterial sheath (Cordis, Fremont, Calif) was placed in the common femoral artery by using percutaneous Seldinger technique and used for advancement of intra-arterial catheters. A 1.67-mm pigtail catheter (Beacon Tip Royal Flush; Cook Medical, Bloomington, Ind) was inserted into the suprarenal abdominal aorta with fluoroscopic guidance (75 kVp, 5 mAs). The location of the renal arteries was determined with DSA by using a 10-mL injection of iodinated contrast agent Omnipaque (iohexol, 350 mg of iodine per milliliter; GE Healthcare, Waukesha, Wis). The pigtail catheter was removed and a custom-made polytetrafluoroethylene

MR-safe guide catheter (2.8-mm outer diameter/2.2-mm inner diameter) (Penumbra) was inserted through the arterial sheath and positioned in the aorta 5 cm inferior to the renal arteries. The MARC catheter was subsequently inserted through the custom guide and advanced until 2 cm of the distal tip extended beyond the guide catheter.

The animal was next moved into the MR suite. MR imaging was performed by using a four-channel surface receive coil (Table 1). Relevant renal anatomy was localized by using an initial survey sequence, after which a high-resolution three-dimensional MR angiogram was acquired by using a 12-mL intravenous injection of gadopentetate dimeglumine (Magnevist; Bayer Healthcare, Whippany, NJ). Image data from the angiography were reformatted into a maximum intensity projection, which was used to prescribe oblique imaging planes for baseline velocity-encoded images of each renal artery. A four-dimensional perfusion imaging was also performed to obtain the baseline perfusion rates for each kidney.

After baseline flow and perfusion imaging, the MARC catheter was advanced into the renal artery by using a real-time balanced steady-state free precession sequence for navigation. A small bolus of dilute intra-arterial gadolinium (1:40 dilution with 0.9% saline)

was injected through the MARC catheter to verify that the tip was successfully located in the renal artery. Embolic agents were then delivered through the MARC catheter while the kidney was imaged by using a real-time two-dimensional MR angiographic sequence.

Embolization Protocol

The embolic agents used in this study were 100–300-μm microspheres (Embosphere; Merit Medical, South Jordan, Utah), packaged as 2 mL of microspheres suspended in 3 mL of 0.9% saline solution. This 5-mL solution was incubated at room temperature with 10 mL of gadolinium-based contrast agent for 72 hours before the endovascular procedure to aid in visualization of the microspheres during MR-guided embolization. Immediately before delivery, another 10 mL of 0.9% saline was added to the gadolinium-containing embolic agent solution for two reasons: (a) to reduce the chance of obstructing the lumen of the MARC catheter with a high concentration of microspheres and (b) to dilute the gadolinium concentration of the solution sufficiently to avoid T_2^* effects during imaging. Four 25-mL doses of embolic agent (2-mL microspheres, 13-mL saline, 10-mL gadolinium) were delivered (S.W.H., D.L.C., M.W.W.) to the kidney during the procedure to ensure complete embolization.

After embolization of one kidney by using the MARC catheter under MR guidance, the animal was moved back to the C-arm suite for contralateral kidney embolization under x-ray guidance. The same custom guide catheter and 3.67-mm introduction sheath used during MR guidance were also used during x-ray guidance. A 0.014-inch guidewire (Synchro-14; Boston Scientific, Marlborough, Mass) was advanced into the contralateral renal artery, and a 0.57-mm catheter (Excelsior SL-10; Stryker Neurovascular, Fremont, Calif) with a 45° angled tip was tracked over the guidewire after which the guidewire was removed. The time taken from the start of navigation to the successful access to the lateral origin of the renal artery was recorded. The metric chosen to compare

Table 1

MR Sequences and Parameters

Sequence	Three-dimensional MR Angiography	Velocity Encoded	Four-dimensional Perfusion	Balanced Steady-State Free Precession	Two-dimensional MR Angiography
Echo time (msec)	1.3	5.0	2.0	1.7	1.4
Repetition time (msec)	4.2	8.0	4.0	3.4	4.3
Flip angle (degrees)	30	15	10	60	30
Field of view (cm)	28 × 28	16 × 16	28 × 28	20 × 20	20 × 20
Frame rate (frames per second)	Not applicable	Not applicable	Not applicable	1.3	0.3
Section thickness (mm)	2	5	4	10	20
No. of sections	100	1	30	1	1
Section orientation	Coronal	Oblique	Coronal	Coronal	Coronal
Cardiac gating	No	Yes	No	No	No
Breath hold	Yes	Yes	Yes	No	No

navigation between the two modalities was catheter navigation time from the aorta into the renal artery origin. Four 25-mL doses of embolic agent solution were then delivered through the catheter, including 10 mL of Omnipaque (iohexol, 300 mg of iodine per milliliter; GE Healthcare) in lieu of gadolinium-based solution. After embolization, a second abdominal aortogram was obtained with the pigtail catheter as mentioned earlier, and the animal was moved back to the MR suite for post-therapy velocity-encoded and perfusion imaging.

Quantitative MR Data Analysis

Analysis of the velocity-encoded MR data was performed (P.V.L., A.J.M., J.K.Y., A.D.L.) by using the QFlow tool on an MR imaging–extended workspace workstation (Philips). Mean flow rates were calculated across 32 cardiac phases for each renal artery, with 80–180 image pixels included in each calculation. The metric chosen to compare the velocity-encoded images was the change in mean renal artery flow rate between that before embolization and that after. Custom Matlab scripts (Mathworks, Natick, Mass) were used to analyze (P.V.L.) the MR data from pre- and postembolization perfusion images. Mean MR signal intensity was calculated for the renal parenchyma (200–300 individual pixels) from the center slice of each kidney for each animal over all time points in the image. The value of the mean MR signal intensity could be influenced by various

factors, including the surface coil sensitivity, volume of gadolinium-based contrast agent delivered, renal clearance rate of gadolinium by the animal, et cetera; hence, the differential of the mean MR signal intensity was computed to use as a comparison metric across animals and modalities. The quantitative metric chosen to compare the perfusion data from the two imaging modalities was the maximum change in perfusion rate between that before embolization and that after embolization.

Euthanasia and Histologic Examination

At the end of each experiment, the animal was euthanized (C.S., M.S., P.V.L.) and both kidneys were extracted, rinsed in saline solution, weighed, and preserved in a tissue fixative (10% buffered formalin phosphate; Fisher Scientific, Waltham, Mass). The weight of each kidney was used to normalize the flow rates from the QFlow analysis. After fixation, each kidney was sectioned axially and hematoxylin-eosin histologic examination was performed (P.V.L.).

Results

In vivo injections of microspheres were successful in all six swine kidneys. Images from the MR protocol are shown in Figure 3. An axial maximum intensity projection from three-dimensional MR angiography (Fig 3a) was used to prescribe the oblique sagittal imaging plane for velocity-encoded flow assessment of

the renal artery (Fig 3b). During MARC catheter navigation under real-time steady-state free precession imaging it was determined that a shallow oblique coronal plane offered the best visualization of the renal artery origin. When activated, the magnetic field from the MARC catheter tip created a local susceptibility artifact, thus allowing the operator to track its position (Fig 3c, 3d). MR-guided navigation into the renal arteries was straightforward for the interventionalists, taking only a slightly longer time than x-ray guided catheterization to achieve similar positions in the main renal arteries. After renal artery catheterization, embolization was performed under real-time visualization (Fig 3e), demonstrating progressive enhancement of the entire renal parenchyma as gadolinium-soaked microspheres lodged in the renal vasculature. Postembolization velocity-encoded images showed a large reduction in flow through the renal artery (Fig 3f).

Images from different portions of the x-ray protocol are shown in Figure 4. The radio-opaque markers in the images are elements from the four-channel surface coil used for MR imaging. This coil was put into position at the start of the procedure, and its position was held constant until all portions of the procedure were concluded. The MARC catheter created unique contrast in the x-ray image due to current-carrying copper wires helically braided within the wall of the catheter.

Figure 3

a.

b.

c.

d.

e.

f.
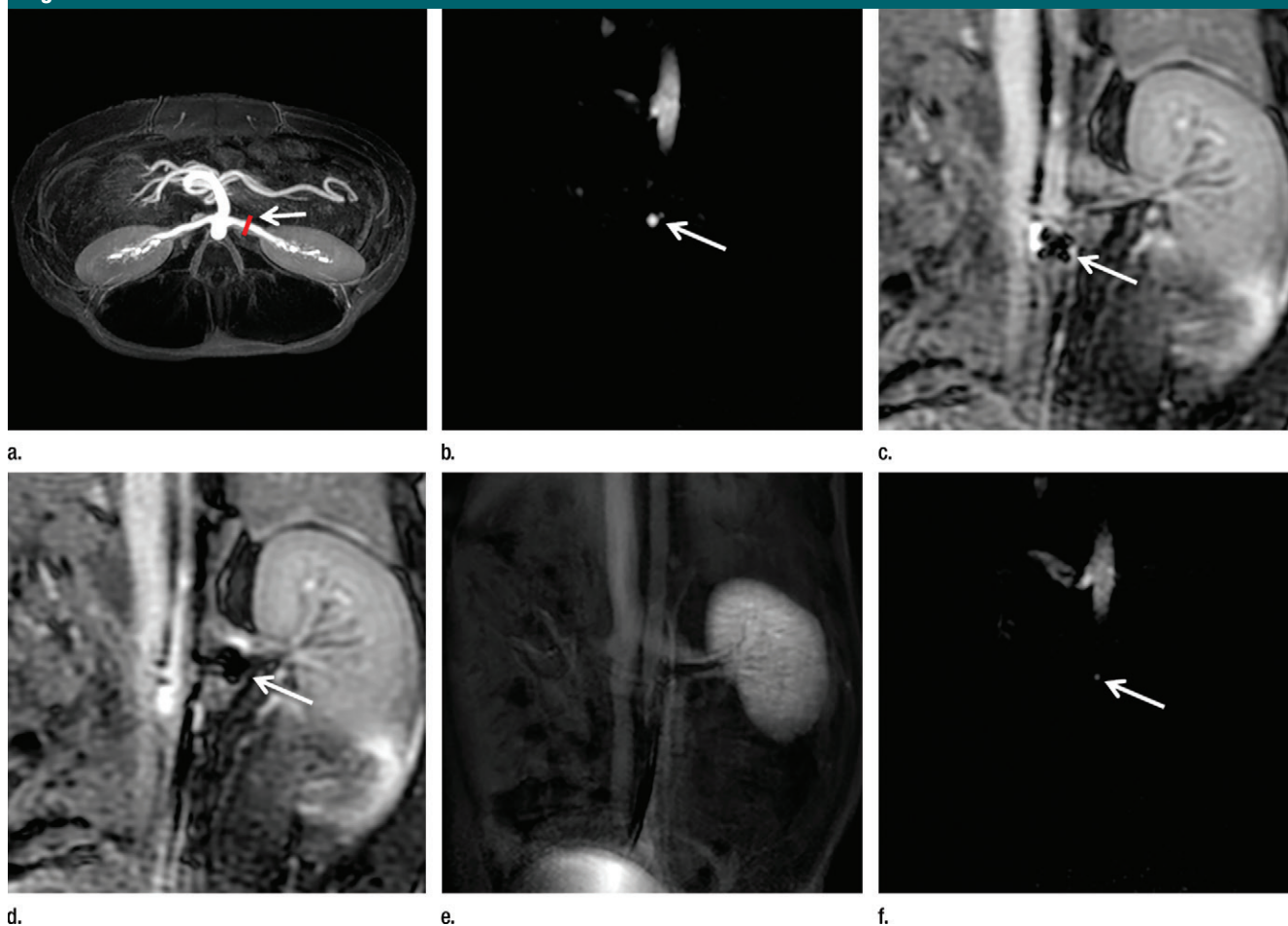
Figure 3:   MR-guided embolization of swine kidney by using the MARC catheter system. **(a)** Axial maximum intensity projection from three-dimensional MR angiography of one of the swine (mean weight, 43 kg ± 2). Arrow = position of the oblique plane perpendicular to the left renal artery that was used for the velocity-encoded image. **(b)** Baseline oblique sagittal velocity-encoded image. Arrow = left renal artery in this plane. Mean flow rates in the renal artery across the 32 cardiac phases were calculated from the pixels in the vicinity of the arrow. **(c, d)** Balanced steady-state free precession images show navigation of the MARC catheter from the aorta into the proximal left renal artery. Arrow = location of the MARC catheter tip. When activated, the magnetic field from the MARC catheter tip created a local susceptibility artifact, allowing the operator to track its position. After successful navigation, embolization was performed. **(e)** Image demonstrates contrast enhancement at 300 seconds into the embolization procedure. **(f)** Postembolization velocity-encoded image shows a large reduction in flow through the renal artery (arrow).

The outline of the right kidney can still be visualized (Fig 4c) due to residual iodinated contrast material from the embolization procedure that could not be cleared by the embolized organ.

Representative histologic samples with hematoxylin-eosin stain from both the x-ray and MR embolization procedures are shown in Figure 5 . No microspheres were present in any of the histologic samples from the control kidney. Histologic samples from kidneys that underwent MR- and x-ray guided embolization all contained microspheres within the renal arterioles.

The mean MR signal intensities and differential of the MR signal intensities for two swine kidneys are shown in Figure 6. As expected, in both the MR and x-ray procedures the pre-embolization perfusion signal in each kidney increased when the gadolinium-enhanced contrast agent was delivered and then reached a steady state value soon after. In the postembolization perfusion images, the signal intensities remain constant because the presence of the embolic agents prevents additional contrast agent from reaching the renal parenchyma. A summary of navigation times, changes in renal artery velocity, and changes in perfusion rates are provided in Table 2.

Discussion

Our study demonstrates feasibility of a simple endovascular intervention by using the MARC catheter system and demonstrates that the current system architecture is compatible with the
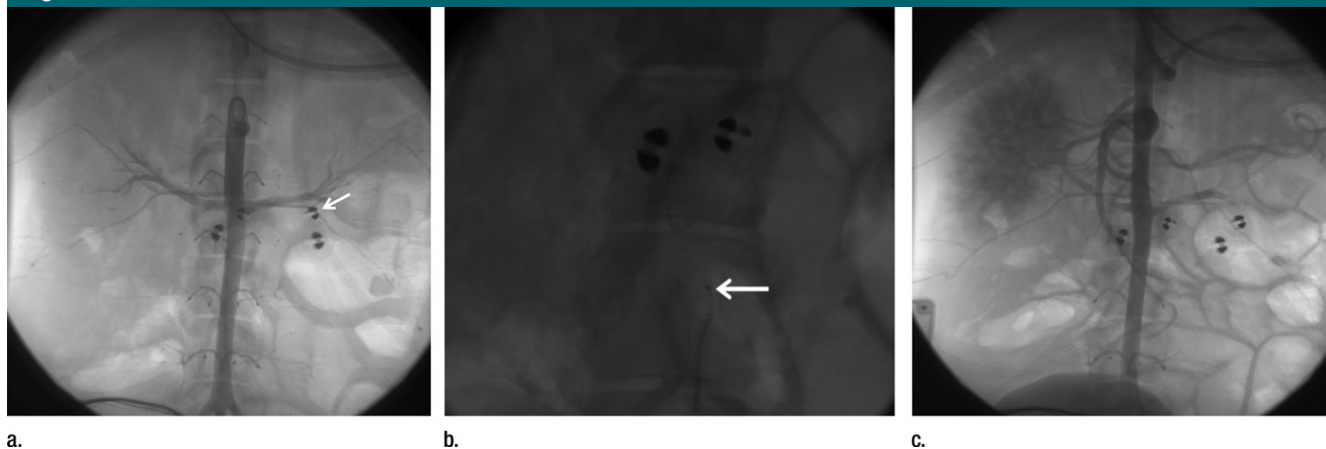
Figure 4: Compilation x-ray images. **(a)** Initial aortogram identifies the positions of both renal arteries after the injection of iodinated contrast agent. Arrow = radiopaque material in the MR surface receive coil. **(b)** Radiograph shows positioning of the MARC catheter tip in the infrarenal aorta (arrow) prior to MR-guided embolization of the left kidney as shown in Figure 3. **(c)** Postembolization aortogram demonstrates contrast agent stasis in both renal arteries and iodinated contrast agent staining the right kidney, as iodinated contrast agent was mixed with embolic agents during x-ray-guided embolization (whereas gadolinium staining of the left kidney is not seen).
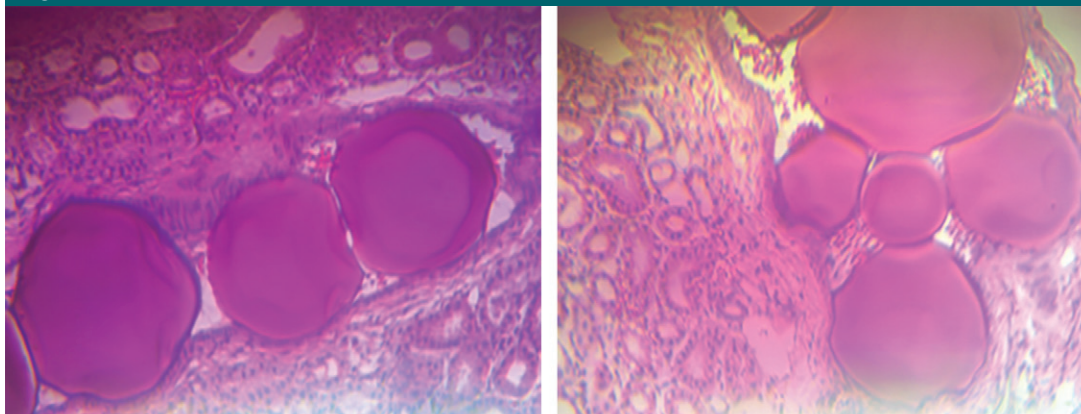
Figure 5: Renal histologic examination. Hematoxylin-eosin–stained images from kidneys that underwent embolization under **(a)** MR and **(b)** x-ray guidance demonstrate microspheres lodged in arterioles.

MR environment in a simulated clinical setting. Use of MR guidance to perform this type of intervention offers the possibility to quantitatively measure success (eg, perfusion change, velocity change) without moving the subject to another imaging modality. Hence, if the result of the procedure is deemed unsatisfactory the operator can quickly re-access the relevant anatomy and continue intervention to improve the outcome. This approach could be particularly valuable in ischemic stroke intervention (wherein serial diffusion-weighted MR images can assess brain parenchymal viability beyond persistently occluded arteries), as well as tumor embolization (wherein recollateralization from nonembolized vessels could be assessed) (33). Potential future applications include the ability to visualize a therapeutic agent in both the target tissue and normal tissue with MR imaging during and immediately after infusion to optimized dose delivery by using novel iron oxide particles bound to chemotherapeutic agents such as superparamagnetic iron oxide (SPIO)-labeled doxorubicin and SPIO-labeled yttrium (34). Compared with contemporary flat-panel computed tomographic (CT) techniques available in modern x-ray angiography suites, MR imaging allows for standard-of-reference evaluation of tissue infarction (eg, diffusion-weighted imaging in stroke therapy), identification of tumors not visible on CT scans (eg, some forms of hepatocellular
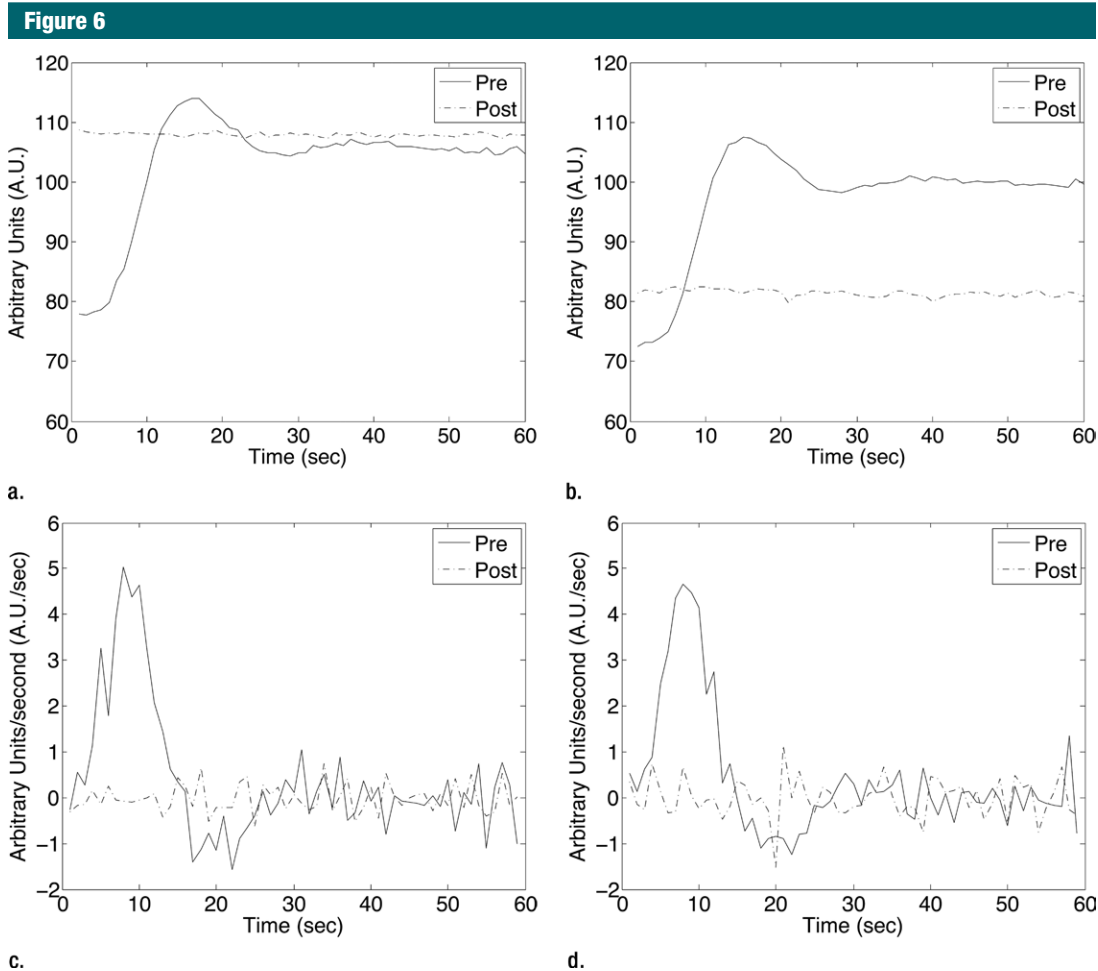
Figure 6

Figure 6: MR perfusion characteristics after x-ray–guided versus MR-guided renal embolization. Graphs show the mean signal intensities for the kidneys embolized under **(a)** MR and **(b)** x-ray guidance. The differentials for the respective mean signals are shown in **c** and **d**.

Table 2

Comparison of Catheter Navigation Time, Perfusion Rates, and Renal Flow Rates

Value	Navigation Time (sec)		Perfusion Rate (au/sec)		Renal Flow Rate (mL/min/g)	
	MR Guidance	X-Ray Guidance	MR Guidance	X-Ray Guidance	MR Guidance	X-Ray Guidance
Mean	93	60	4.9	4.6	2.1	1.9
Standard deviation	56	22	0.5	0.6	0.2	0.2
Median	67	53	5.0	4.9	2.1	1.9
Minimum	54	42	4.4	3.9	1.9	1.8
Maximum	157	85	5.5	5.1	2.2	2.1

carcinoma), and the potential for iterative intraprocedural physiologic evaluations (eg, tissue perfusion analysis) as therapy progresses that would be unappealing using flat-panel CT given the large amount of ionizing radiation

associated with repeated flat-panel CT examinations.

Although considerable progress has been made, there are still significant limitations of MR guidance relative to x-ray guidance for the

embolization procedure assessed. MR guidance required more navigation time and had increased variability, compared with x-ray guidance in our study. This could be related to the decreased temporal and spatial

resolution when using MR guidance relative to x-ray, buckling of the MARC catheter during insertion into renal artery causing the operator to perform multiple insertions, the larger outer diameter of the MARC catheter used for MR-guided catheterization compared with the SL-10 catheter used for x-ray guided catheterization, and the operator having a better ergonomic environment in the C-arm suite. The size, stiffness, and method of mechanical attachment of the alumina tip of the MARC catheter all influence the mechanical properties of the catheter and can make it more challenging to advance into the renal artery than commercial microcatheters that have been mechanically optimized for guidewire-assisted x-ray–guided intervention over several decades. The friction between the MARC tip and the renal artery wall just beyond the renal artery origin can cause buckling of the MARC catheter body, thus preventing catheter advancement.

The lack of MR-compatible guidewires on the market exacerbates the issue of friction because a guidewire could be used in conjunction with the MARC catheter to temporarily increase the stiffness of the catheter body when advancement is necessary. Recent efforts to develop commercially viable 0.014-inch and 0.035-inch MR-compatible and visible polymer guidewires are encouraging and will facilitate MR-guided endovascular interventions using the MARC system as well as nonmagnetic MR-safe catheters (35). This issue may also be solved by further miniaturization of the MARC catheter tip and/or iterating the design so that the microcoil is embedded within the catheter itself similar to the copper current-carrying wires.

We performed procedures in a terminal vascular system with little or no collateralization. The renal vasculature was selected in this study because it represents a simple embolization model for early studies. The internal diameter of the MARC catheter limited the size of embolic microspheres in

our study. The perfusion rate and renal flow rate differences before embolization and after embolization, however, were comparable between the two imaging modalities, indicating effective embolization under each guidance modality. Future studies in more complex vascular systems, such as the uterine vasculature, can further evaluate real-time MR imaging capabilities in adequately detecting competing and collateral flow during use of particulate, coil, or liquid embolic agents.

The primary limitation of our study is a small sample size. Due to the small number of animals used in our study, there is not sufficient statistical power to claim significance for quantitative differences between x-ray and MR imaging guidance. However, it is possible to use these data as a pilot study to compute a prospective sample size necessary to perform hypothesis testing with sufficient statistical power. For example, a sample of $n = 25$ would be required to claim a statistical difference between MR and x-ray navigation times with 80% power. Similarly, whereas a sample of $n = 10$ would be needed to claim a statistical difference in renal artery flow rates at 80% power, a sample of $n = 58$ would be required for analysis of renal parenchymal perfusion. It is expected that flow rate would require the smallest sample size since it had the smallest relative variation in the measurement.

In conclusion, our study demonstrates the feasibility of using the MARC catheter in MR-guided endovascular embolization and opens up a novel opportunity to perform endovascular procedures in the MR imaging environment, wherein the interventionalist has direct access to intraprocedural imaging biomarkers of physiology. These immediate quantitative results from MR velocity and perfusion data can determine the effectiveness of the intervention. For clinical translation, several aspects of the system can be improved including mechanical design of the catheter tip and the ergonomics of the interventional environment in the MR suite.

References

1. Bock M, Wacker FK. MR-guided intravascular interventions: techniques and applications. J Magn Reson Imaging 2008;27(2):326–338.

2. Kos S, Huegli R, Bongartz GM, Jacob AL, Bilecen D. MR-guided endovascular interventions: a comprehensive review on techniques and applications. Eur Radiol 2008;18(4):645–657.

3. Saeed M, Hetts SW, English J, Wilson M. MR fluoroscopy in vascular and cardiac interventions (review). Int J Cardiovasc Imaging 2012;28(1):117–137.

4. Ratnayaka K, Faranesh AZ, Guttman MA, Kocaturk O, Saikus CE, Lederman RJ. Interventional cardiovascular magnetic resonance: still tantalizing. J Cardiovasc Magn Reson 2008;10:62.

5. Atalar E, Kraitchman DL, Carkhuff B, et al. Catheter-tracking FOV MR fluoroscopy. Magn Reson Med 1998;40(6):865–872.

6. Sequeiros RB, Ojala R, Kariniemi J, et al. MR-guided interventional procedures: a review. Acta Radiol 2005;46(6):576–586.

7. Henk CB, Higgins CB, Saeed M. Endovascular interventional MRI. J Magn Reson Imaging 2005;22(4):451–460.

8. Saeed M, Saloner D, Weber O, Martin A, Henk C, Higgins C. MRI in guiding and as-

sessing intramyocardial therapy. Eur Radiol 2005;15(5):851–863.

9. Wacker FK, Hillenbrand CM, Duerk JL, Lewin JS. MR-guided endovascular interventions: device visualization, tracking, navigation, clinical applications, and safety aspects. Magn Reson Imaging Clin N Am 2005;13(3):431–439.

10. Schulz T, Tröbs RB, Schneider JP, et al. Pediatric MR-guided interventions. Eur J Radiol 2005;53(1):57–66.

11. Rickers C, Jerosch-Herold M, Hu X, et al. Magnetic resonance image-guided transcatheter closure of atrial septal defects. Circulation 2003;107(1):132–138.

12. Atalar E, Ménard C. MR-guided interventions for prostate cancer. Magn Reson Imaging Clin N Am 2005;13(3):491–504.

13. Blanco Sequeiros R, Carrino JA. Musculoskeletal interventional MR imaging. Magn Reson Imaging Clin N Am 2005;13(3):519–532.

14. Nour SG, Lewin JS. Radiofrequency thermal ablation: the role of MR imaging in guiding and monitoring tumor therapy. Magn Reson Imaging Clin N Am 2005;13(3):561–581.

15. Wendt M, Wacker FK. Visualization, tracking, and navigation of instruments for magnetic resonance imaging-guided endovascular procedures. Top Magn Reson Imaging 2000;11(3):163–172.

16. Zuehlsdorff S, Umathum R, Volz S, et al. MR coil design for simultaneous tip tracking and curvature delineation of a catheter. Magn Reson Med 2004;52(1):214–218.

17. Dumoulin CL, Souza SP, Darrow RD. Real-time position monitoring of invasive devices using magnetic resonance. Magn Reson Med 1993;29(3):411–415.

18. Rube MA, Holbrook AB, Cox BF, Houston JG, Melzer A. Wireless MR tracking of interventional devices using phase-field dith-

ering and projection reconstruction. Magn Reson Imaging 2014;32(6):693–701.

19. Kuehne T, Fahrig R, Butts K. Pair of resonant fiducial markers for localization of endovascular catheters at all catheter orientations. J Magn Reson Imaging 2003;17(5):620–624.

20. Carias M, Hynynen K. The evaluation of steerable ultrasonic catheters for minimally invasive MRI-guided cardiac ablation. Magn Reson Med 2014;72(2):591–598.

21. Miles RR, Schumann DL, Pearson MA, Hilken D. Steerable catheter with distending lumen-actuated curling catheter tip. Google Patents, 2010.

22. Mather PT, Luo XF, Rousseau IA. Shape memory polymer research. Annu Rev Mater Res 2009;39:445–471.

23. Lalande V, Gosselin FP, Martel S. Catheter steering using a magnetic resonance imaging system. Conf Proc IEEE Eng Med Biol Soc 2010;2010:1874–1877.

24. Gosselin FP, Lalande V, Martel S. Characterization of the deflections of a catheter steered using a magnetic resonance imaging system. Med Phys 2011;38(9):4994–5002.

25. Gudino N, Heilman JA, Derakhshan JJ, Sunshine JL, Duerk JL, Griswold MA. Control of intravascular catheters using an array of active steering coils. Med Phys 2011; 38(7):4215–4224.

26. Lillaney P, Caton C, Martin AJ, et al. Comparing deflection measurements of a magnetically steerable catheter using optical imaging and MRI. Med Phys 2014;41(2): 022305.

27. Losey AD, Lillaney P, Martin AJ, et al. Magnetically assisted remote-controlled endovascular catheter for interventional MR imaging: in vitro navigation at 1.5 T versus X-ray fluoroscopy. Radiology 2014;271(3):862–869.

28. Hetts SW, Saeed M, Martin AJ, et al. Endovascular catheter for magnetic navigation under MR imaging guidance: evaluation of safety in vivo at 1.5T. AJNR Am J Neuroradiol 2013;34(11):2083–2091.

29. Demas V, Herberg JL, Malba V, et al. Portable, low-cost NMR with laser-lathe lithography produced microcoils. J Magn Reson 2007;189(1):121–129.

30. Moftakhar P, Lillaney P, Losey AD, et al. New-generation laser-lithographed dual-axis magnetically assisted remote-controlled endovascular catheter for interventional MR imaging: in vitro multiplanar navigation at 1.5 T and 3 T versus x-ray fluoroscopy. Radiology 2015;277(3):842–852.

31. Sincic RS, Caton CJ, Lillaney P, et al. System architecture for a magnetically guided endovascular microcatheter. Biomed Microdevices 2014;16(1):97–106.

32. National Research Council. Guide for the care and use of laboratory animals. 8th ed. Washington, DC: The National Academies Press, 2011.

33. Wang D, Gaba RC, Jin B, et al. Perfusion reduction at transcatheter intraarterial perfusion MR imaging: a promising intraprocedural biomarker to predict transplant-free survival during chemoembolization of hepatocellular carcinoma. Radiology 2014; 272(2):587–597.

34. Li W, Zhang Z, Gordon AC, et al. SPIO-labeled yttrium microspheres for MR imaging quantification of transcatheter intrahepatic delivery in a rodent model. Radiology 2016;278(2):405–412.

35. Düring K. Novel MR safe guidewires for MRI-guided interventions. Interventional MRI Symposium, Leipzig, Germany, 2014; 30.